

Effects of Axial Leakage on Torque Performance in PM Machines

J. Engström

ITT Flygt AB
Box 1309, 171 25 Solna, Sweden
jorgen.engstrom@flygt.com

Abstract - This paper examines the effect of axial leakage in electrical machines with special attention to the torque production in slotless machines. The analysis is carried out by means of three-dimensional (3D) finite element calculations. The outcome of the analysis show that for slotless machines, the torque reduction due to axial leakage is negligible.

Keywords: slotless machine, airgap winding, 3D-FEM, axial leakage

1. Introduction

In the design of electrical machines in general, the calculation of its performance is usually restricted to a 2D analysis, i.e. the effects of any axial leakage is discarded. This manner is justified in many cases because of the small airgap in conventional machines. A study of the axial leakage in motors with buried magnets can be found in [1].

There are however cases where the effects of axial leakage might have a larger influence. Such a case is slotless machines, where the airgap length is significantly larger than in conventional machines. And, if the performance deviates from what is predicted by the 2D models, these models must be revised or correction factors introduced. 2D models for slotless PM machines can be found for example in [2].

The aim of this paper is therefore to investigate the influence of axial leakage in slotless PM machines. The investigation is restricted to radial flux machines with surface mounted magnets. The theoretical analysis is carried out by means of a 3D-FEM software¹. The results of this analysis is compared to measurements on a prototype machine.

2. 3D modelling

The principal outline of the geometry used in this investigation is shown in Fig. 1.

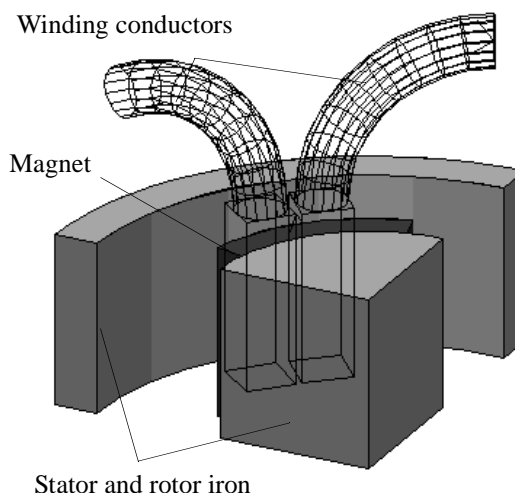


Fig. 1 Geometry used for the FEM calculations, winding shown as wire frames.

The stator winding currents are applied using a certain function of the Flux3D which enables the user to define regions where the current is flowing. These regions are not a part of the geometry and are thus not meshed. The winding regions are pictured in Fig. 1 as wire frames.

As only the comparison between the torque obtained by 2D and 3D analysis is of interest here, there is no need to model the complete winding of the machine. Instead, the winding is represented by two conductors placed in the middle of the airgap, representing one winding phase. The conductor cross section covers most of the winding area of one phase, which means that the representation of one phase is justified. As the three phase winding is symmetrical, the omission of two phases decreases the torque by a factor, but does not affect the comparison between 2D- and 3D-torque calculation.

The iron material is assumed to be linear (no saturation). The magnet is modelled as a one-piece arc-shaped magnet with radial magnetisation. In reality, the magnet consists of a number of rectangular pieces with parallel magnetisation, but this has a minor influence on the result.

1. Flux3D by Cedrat

3. Illustrations of the axial leakage flux

One example of the flux density at the stator surface when axial leakage is present is shown in Fig. 2.

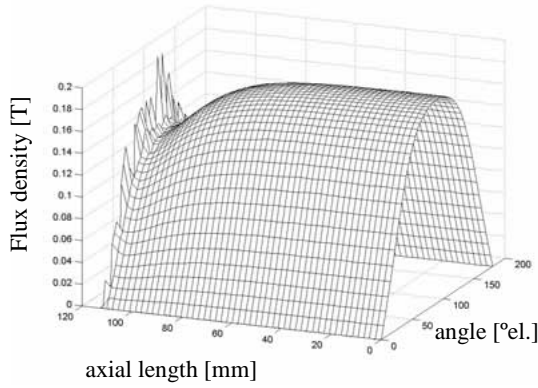


Fig. 2 Surface showing airgap flux density at the stator surface (one pole)

The active length of the machine is 225 mm, the picture is showing half of the machine. As can be seen, the surface is very smooth (due to the large airgap). If the fundamental component of flux density is examined at different radii, the result is as shown in Fig. 3 below.

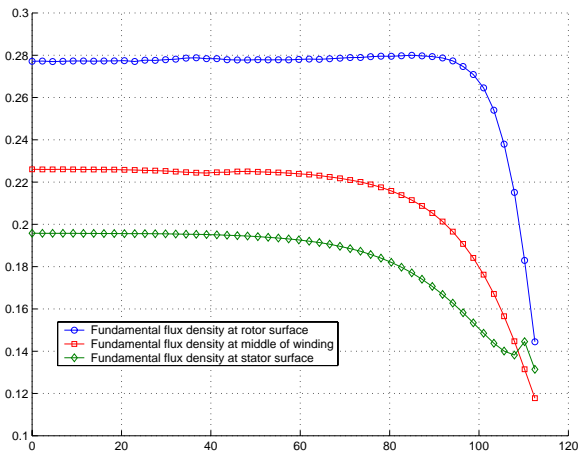


Fig. 3 Fundamental component of the radial flux density at different radii.

To get an idea of how the paths of leakage flux is oriented in the end winding region, the following analysis was made. An “observation” surface was applied to the geometry at the middle of one pole according to Fig. 4.

This surface covered both the end winding region and a part of the motor geometry. Then the flux density vectors were plotted along this surface. This plot is shown in Fig. 5.

It can be noticed that a substantial part of the leakage flux returns to the stator via the end winding region.

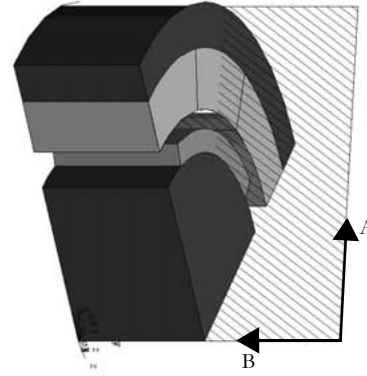


Fig. 4 Definition of the surface for leakage flux examination in Fig. 5.

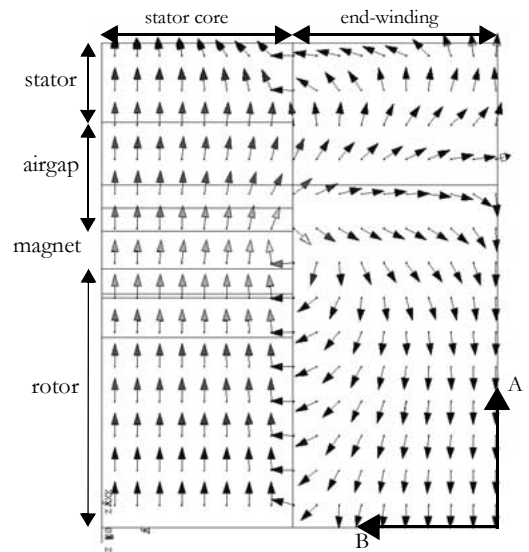


Fig. 5 Arrows showing direction of flux in the end winding region and the motor body.

4. Results of the 3D-calculation

A Influence of airgap geometry

To evaluate the decrease of torque due to axial leakage, the calculation of torque by 3D-analysis was compared to the result of the 2D-calculation. A coefficient of this loss of torque is defined as the quotient of the torque obtained by 3D analysis (T_{3D}) and the 2D torque (T):

$$k_T = \frac{T_{3D}}{T} \quad (1)$$

At first, the influence of the geometry of the airgap was investigated. In this case, the analysis is carried out for four pole machines. Three different geometries was used which parameters are shown in Table 1.

Geometry I corresponds to the prototype machine used for measurements. Geometry II has a larger airgap length

TABLE 1 - Parameters for the investigated geometries

Geometry	I	II	III
airgap length	44	63	25
rotor radius	79	60	98
magnet thickness	10	10	8

and geometry III has a smaller airgap length. In all cases, the winding conductors were placed in the middle of the airgap.

For all three geometries, the torque loss coefficient was calculated for a number of different rotor lengths. The result of these calculations are shown in Fig. 6 below.

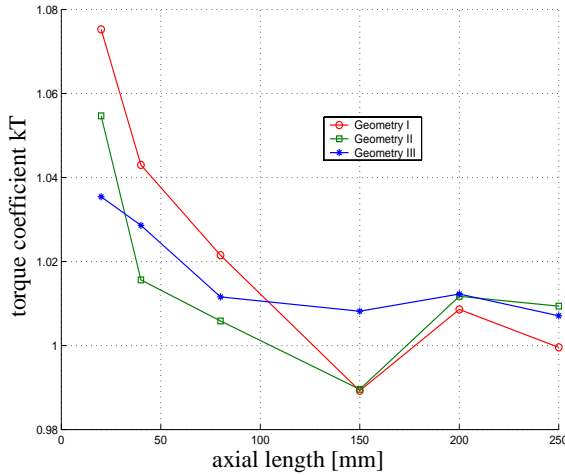


Fig. 6 Torque coefficient for the four pole geometries as a function of rotor length.

The results show that very little torque is lost, which was first surprising. Furthermore, for short machines, the torque is higher than expected from 2D analysis.

The explanation for this is that leakage flux is linked by the end winding. When the results were further examined, it was found that the torque developed in the winding within the core volume was lower due to the leakage, as expected. But the torque developed in the end winding was found to compensate this loss of torque.

To illustrate this further, the flux density and torque along the conductors were examined. In Fig. 7 below, an analysis of the flux density (radial component) and torque of a 225 mm long machine is shown

The curves in Fig. 7 are evaluated along a line placed in the middle of one of the coils. This line follows the straight part of the coil but not the end winding coil; the line continues in the axial direction. The dashed lines corresponds to the case of no axial leakage.

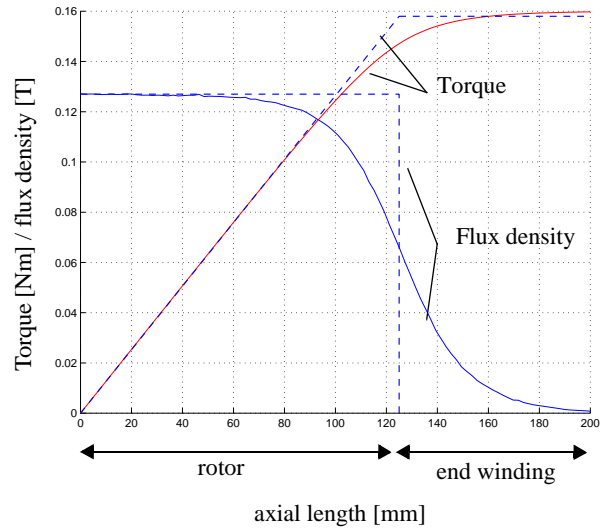


Fig. 7 Airgap flux density and torque production for the cases of no leakage (dashed lines) and with leakage (solid lines)

As can be seen in the figure above, the flux density in the middle of the machine is the same as without leakage and close to the end the level has decreased by about 50%. The torque line in Fig. 7 is calculated as the integral of the flux density, which is used as a measure of the torque. This line thus illustrates the torque as a function of the conductor length.

If the conductor has the same length as the rotor (125 mm in the figure) the torque is lower than what would be achieved without axial leakage. But if the conductors are made longer than the machine, the resulting torque increases; it can even be slightly higher than the 2D torque if the conductors are long enough. As the end windings normally are arranged in such way that they first continue axially and then gradually divert to another direction, the radial component of the leakage flux passing the end-windings contributes to the torque production. The result is that the torque will be approximately the same as calculated by 2D-analysis.

In Fig. 7, the conductor coil is assumed to lie only in the axial direction, which is not the case of the actual end windings. This means that the torque contribution from the outer most part of the conductor is exaggerated. This does not however change the situation.

B Influence of pole number

The influence of pole number was also analysed. The torque coefficients for two and six poles were examined and compared to four pole geometry. The same dimensions as

for geometry I above was used. The result of the comparison is shown in Fig. 8.

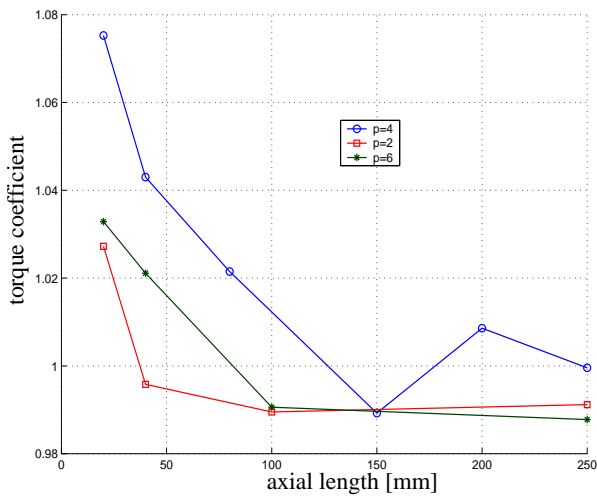


Fig. 8 Comparison of torque coefficients for different pole numbers.

As can be seen, there is no significant difference in the torque coefficient between these pole numbers. Possibly the four pole machine has slightly higher torque, especially for short machines.

C Influence of winding configuration

The case of having a toroidal winding was also examined. In this type of winding, the end coils are placed on the back of the stator core, i.e. the winding is wound around the stator core as shown in Fig. 9 (one phase shown).

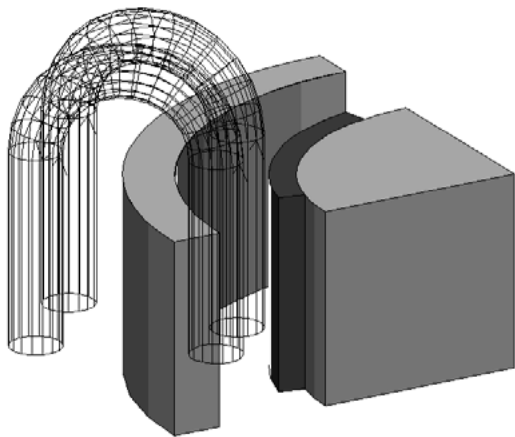


Fig. 9 Geometry for toroidal winding geometry

The torque coefficient for the toroidal winding was compared to the “normal” winding for a four pole geometry and the result is presented in Fig. 10.

As can be observed in Fig. 10, the torque coefficient for toroidal windings is below unity (an infinitely long machine will probably have a coefficient close to unity). The torque coefficient decreases for shorter machines, which implies

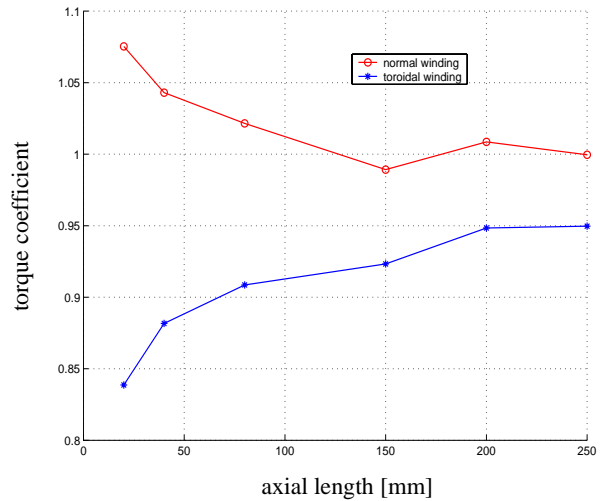


Fig. 10 Comparison of torque coefficients for normal and toroidal windings.

that in this case the torque produced in the end windings is low.

5. Measurements

The verification of the above results was made by measuring both the torque and no load voltage of the machine. The measurements revealed a discrepancy between the calculated and measured values, see Table 2.

TABLE 2 - Difference between calculated and measured values of EMF and torque

	Calculated	Measured	Discrepancy
EMF	238	224	5.9%
Torque	69	64	7.2%

This was at first discouraging. However, direct measurements of the airgap flux density by means of a Hall sensor probe¹ gave another picture. The probe was placed at a distance above the magnets of approximately 7 mm. The result of the measurement is shown in Fig. 11 below. In the pictured measurement the probe was placed in the middle of the rotor axial length and the rotor was rotated while the values were recorded.

As there are four poles in the machine, four peaks in the flux density is visible in the FEM-calculated curve. For the measured values, only the peak values were recorded.

In this figure, two interesting phenomena can be seen. First of all, the measured overall level is lower than expected. Secondly, one pole seems to create lower flux density than the other three. Both of these effects can be explained by deterioration of the magnets due to thermal cycling when mounting the magnets to the rotor. A more complete discussion of this can be found in [2].

1. F. W. Bell 9200

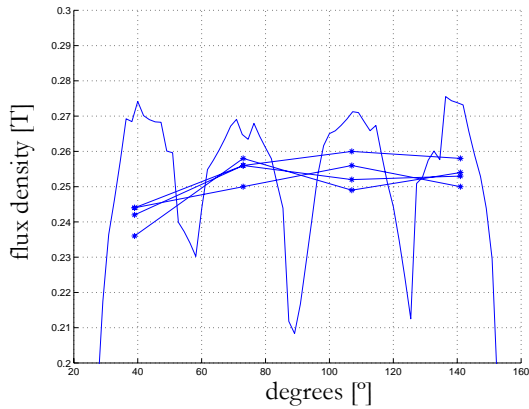


Fig. 11 Measured and FEM calculated values of the airgap flux density close to the rotor.

The measurement was repeated for three positions along the rotor: pos. 1 as described above, pos.3 at the end of the rotor and pos. 2 in between. The result is shown in Table 3 together with the expected values achieved from FEM. The measured values are the average for each position.

TABLE 3 - Measured flux density compared to FEM

Position	Meas.	FEM	quot.
1	0.25	0.27	0.93
2	0.26	0.27	0.96
3	0.23	0.25	0.92
average	-	-	0.94

Despite the inaccuracies related to the measurements, it is concluded that the major part of the discrepancy between calculated and measured torque (see Table 2) derives from the lower flux density. Thus the conclusions regarding the effect of axial leakage still holds.

6. Conclusions

The result of this analysis points out a important difference between slotless and slotted machines. In slotted machines, the end windings are of no or little use. On the contrary, in slotless machines the end windings contribute to the torque production to a great degree.

The consequence is that the torque of slotless machines is almost unaffected by axial leakage. An exception is the case of toroidal winding, where a substantial decrease of torque is found, at least for shorter machines.

Acknowledgements

The research of this paper has been conducted within the Permanent Magnet Drives program at the Competence Centre in Electric Power Engineering, Royal Institute of Technology, Stockholm, Sweden.

References

- [1] Thelin, P., Nee, H.-P., "Analytical Calculation of the Air-gap Flux Density of PM Synchronous Motors with Buried Magnets including Axial Leakage, Tooth and Yoke Saturation, Proc. Eight International Conference on Power Electronics and Variable Speed Drives 2000, PEVD 2000, London, England 2000, pp.218-223.
- [2] Engström, J., "Analysis and Verification of a Slotless Permanent Magnet Motor for High Speed Applications", PhD-thesis, Royal Institute of Technology, Electrical Machines and Power Electronics, Stockholm 2001, ISBN 91-7283-130-8.